Bachelor Thesis

Observations of High Proper Motion Stars

Daniel Milošić
Matriculation No.: 01410127

Karl-Franzens-Universität Graz
Institute of Physics / IGAM

Supervisor: Dr. Thorsten Ratzka

August 2018

Contents

Abstract

The subject of this Bachelor thesis is the proper motion of stars. It serves as a brief introduction to astrometry and describes a practical measurement as well. Using a 50cm-Cassegrain-Telescope at Lustbühel Observatory the exact positions of high proper motion stars were measured and compared to archival data. From these data the relative distances and velocities of the stars were calculated and again compared to the values known from the Hipparcos and Gaia missions. The results agree with the satellite data.

1. Introduction

1.1. Astrometry

Astrometry is a branch of astronomy, that deals with the exact positions and motions of celestial objects. It helped open up important fields of science and gave understanding for the earth's motion through space, the solar system and the galaxy. Currently, Astronomy benefits from technological progress in imaging devices and space flight. By placing large telescopes above the earth's atmosphere, astrometric measurements can be significantly improved.[1]

Distances between two objects across the celestial sphere can be expressed in terms of the angle, which the observer sees between them. Now that we have a definition of distance on this two-dimensional frame, we can define a coordinate system to express the positions of celestial objects. There are many such coordinate systems of the night sky. In this Bachelor thesis the equatorial system is used. It consists of two coordinates, the declination δ and the right ascension α. As a base circle it uses a projection of the earth's equator on the sky. On this circle the declination equal to zero. On the celestial north pole the declination is equal to 90° and on the south pole -90°. The right ascension is the distance to the vernal equinox, ϒ. The declination is divided into 180°, which are divided into 60', which consist of 60''. The right ascension is divided into 24h, each h into 60m, and those again into 60s. This means, 1s in right ascension is equal to 15'' in declination at the equator. When we move away from the equator, we need to multiply the right ascension by cos(δ) to take the projection into account. There are other celestial coordinate systems, e.g. The horizontal system, the ecliptic system and the galactic system, which all work in a similar way.[2]
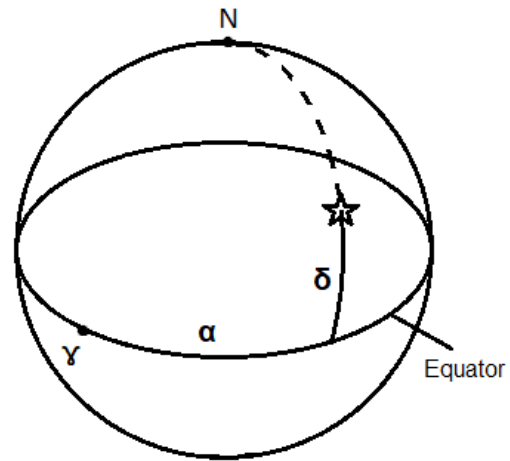

Fig. 1.1: The equatorial coordinate system

In this Bachelor thesis we want to calculate proper motions of stars, meaning velocities across the sky, by comparing their exact positions at different times. With these data we can calculate the differences of the position of the star and use the Pythagorean theorem to find the total distance between the two positions:

$$d = \sqrt{(d_\alpha \cdot cos(\delta))^2 + d_\delta{}^2}$$

Here d_α and d_δ are the differences in declination and right ascension between two epochs, not the uncertainties. We also had to multiply the right ascension with a cos(δ) to compensate for the spherical geometry. Of course, the Pythagorean theorem only applies to flat geometry, but since the angles are very small this can be neglected. For larger angular distances the law of sines should be used instead. With the total distances and the dates, we can now find the velocity:

$$v = \frac{d}{t}$$

---

[1] (Perryman M. , 2012)
[2] (Hanslmaier, 2014)

Exact positions of stellar objects can also be used to determine their distance to earth. This is done by using the parallax angle. The position of the same object is measured twice as seen in Fig. 1.2. The time difference between these measurements is ideally half a year. The closer this object is to earth, the more will its position on the sky change. The half angular distance between these two positions is called the parallax angle. It is therefore inversely proportional to the distance to the object for the small angles found in stellar astronomy. A convenient unit of distance in Astronomy is the parsec. It is the distance of an object, that would have a parallax angle of 1 arc second (equal to 1'' in declination) using 1 Astronomical Unit as basis. 1 Astronomical Unit (AU) is equal to the distance from the earth to the sun. The other way around, 1 AU appears as 1'' in 1pc distance.[1]

Through the motion of the earth around the sun nearby objects appear to perform a circular motion, which is called parallax motion. This is not the only motion that can be observed. The objects themselves often have a high velocity in space in relation to earth. The resulting movement across thy sky is called proper motion, which is the topic of this thesis. Fig. 1.2 shows both the parallax motion and the linear proper motion, which add up to a spiral. As additional component the motion around the center of gravity caused by a planet orbiting the star is shown.[1]
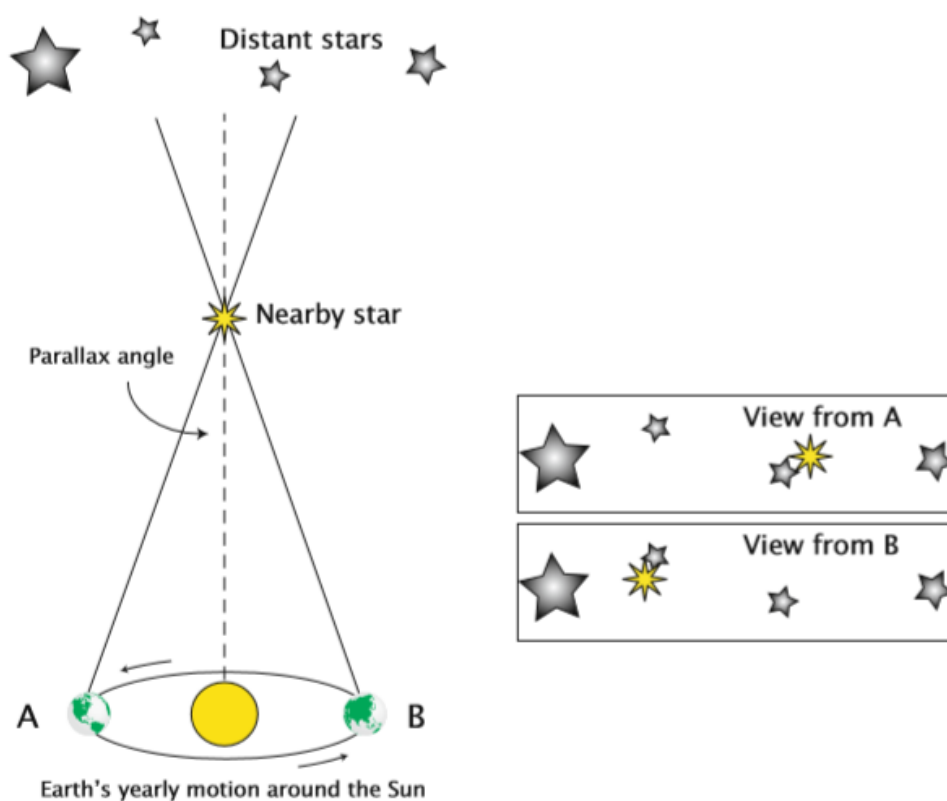

Fig. 1.2: The parallax angle visualized[3]
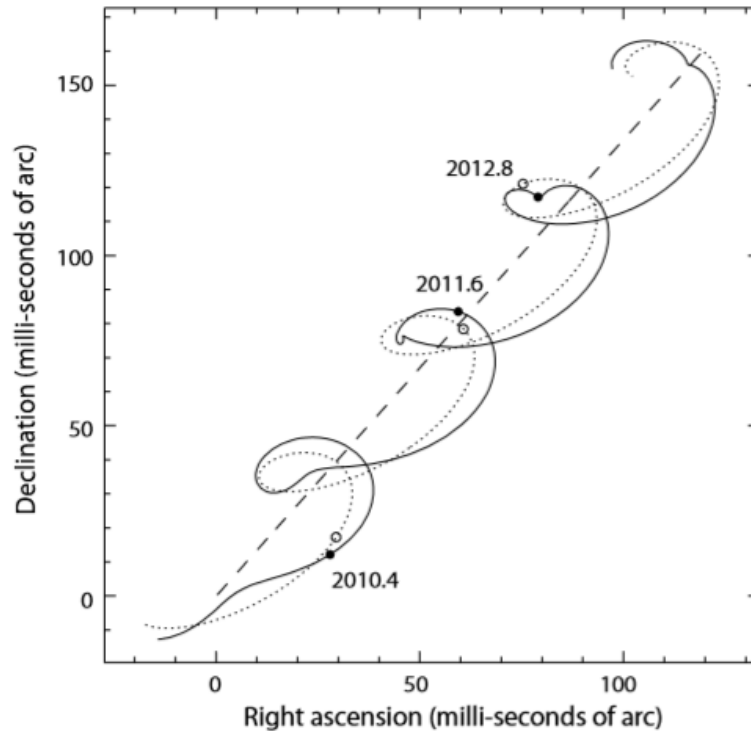
[3] (Perryman M. , 2012)

Fig.1.3: The parallax motion and proper motion of a star. The dashed line shows only the linear motion of a star. The dotted line represents the apparent motion of the star due to the earth rotation around the sun, superimposed with the linear motion from the dashed line. The solid line is the result of these two motions and a more complex motion of a star-planet system, orbiting a common center of mass.[4]

1.2. Surveys

To retrieve the positions of objects at different times, certain sky surveys were used. The first and second generation of the Digital Sky Survey (DSS1 and DSS2) and the Two Micron All Sky Survey (2MASS) were used.

The Space Telescope Science Institute (STScI) published both generations of DSS after retrieving the data from photographic plates. The original plates of the first generation contained 14000 by 13999 square pixels, where the side of each pixel corresponds to 1.70'' of the night sky. These were later divided into smaller blocks and digitally compressed by a factor of 10. After the compression of 600 Gigabytes of images, the data were made available on 100 CD-ROMS in 1994.[5]

The second generation of DSS used plates with a pixel size of 1.0'' x 1.0'', covering the whole celestial sphere in at least 3 band passes. The survey was completed in 2006.[6,7]

The images for 2MASS were gathered between June 1997 and February 2001 and amounted to 25.4 Terabytes of data. They cover 99.998% of the night sky in the near infrared J, H and K_s band passes. 2MASS collected images with a pixel size of 2.0'' x 2.0'' with an integration time of 7.8 s. [8]

---

[4] (Perryman M. , 2012)
[5] (Morrison, 1995)
[6] (Mikulski Archive for Space Telescopes, 2018)
[7] (McLean et al., 2000)
[8] (M.F. Skrutskie et al., 2006)

1.3. The Gaia Mission

Gaia is a spacecraft, built by the European Space Agency (ESA), designed to obtain extremely accurate spectroscopic and astrometric data of celestial objects. It forwards our physical knowledge about various topics, such as star formation, evolution of stars and galaxies, exoplanets, binaries and multiple stars and many more. Gaia is the successor mission to Hipparcos, which influenced many areas of astronomy and measured the absolute parallax of 117955 objects with milli-arcsecond accuracy. Gaia's accuracy is in the order of micro-arcseconds. It was launched in December 2013 and the processing and analysis of the mission data is done by the Data Processing and Analysis Consortium (DPAC).[9]

The main goal of Gaia is to give insight into the origin, structure and dynamics of our galaxy, the Milky Way. Although Gaia measures over a billion stars, this only makes up approximately 1% of the galaxy. It will, however, cover most of its volume. With such a big number of objects Gaia finds stars in numerous phases, contributing to the knowledge about stellar evolution. It is also used for identifying binaries and multiple stars by measuring their proper and parallactic motions. Furthermore, Gaia data can be used to calculate the masses of exoplanets.[7]

This is a schematic view of the spacecraft:
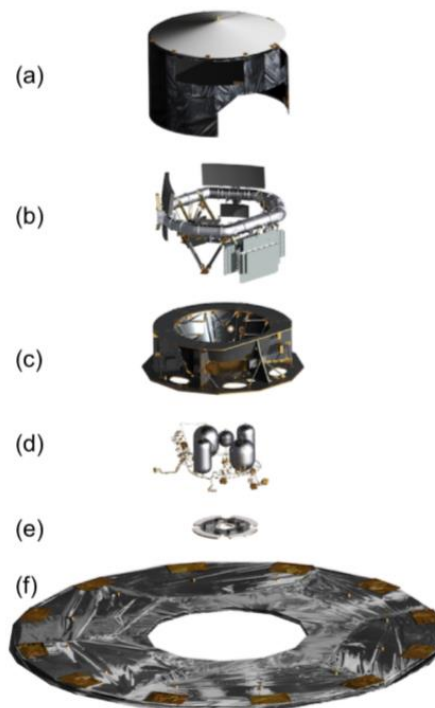
*Fig.2: Schematic view of Gaia. **a)** Payload thermal tent; **b)** payload module: optical bench, telescopes, instruments, and focal plane assembly; **c)** service module (structure): also housing some electronic payload equipment, e.g. clock distribution unit, video processing units, and payload data-handling unit; **d)** propellant systems; **e)** phased-array antenna and f) deployable sunshield assembly, including solar arrays. [10]*

---

[9] (Gaia Collaboration et al., 2016)
[10] (Gaia Collaboration et al., 2016)

2. Measurement

The positions of the stars were determined by taking images of the chosen stars using a 50cm reflecting telescope of the type Cassegrain at Lustbühel Observatory (OLG). It has 500mm aperture, which is also the optical diameter of the primary mirror. The secondary mirror has an optical diameter of 175mm. The available field of view of the telescope is 61 arcminutes and the telescope's focal length is 4500mm. The telescope has an f-ratio of f9 and a back focus of 410mm. The camera's CCD chip has a size of 17.96 x 13.52 mm resulting in a field of view of 13.72' x 10.33'.

2.1. Selection of Stars

Since the accuracy of the instruments and methods at hand cannot compete with the high accuracy of satellite images the stars had to match certain criteria. Frist of all they had to be visible in the night sky on the northern hemisphere in winter. Ideally, they would be located close to the zenith at the time of observation, because of the light pollution of Graz and the better seeing and lower extinction at higher elevation. Furthermore, the apparent magnitude had to be considered. If the brightness were too high, the camera would be saturated, and the exact position would be hard to determine. If instead the star would be very faint, the star might be hard to detect. The most important criterium was the proper motion. The higher the proper motion, the more accurate the results. The stars were chosen from the Hipparcos catalogue[11]. The stars, that were selected are in Table 2.1. The identifiers 1.1 and 1.2 stand for two stars in the double star system.

---

[11] (Perryman M. A., 1997)

Table 2.1: Observed stars

Nr.   … Identifier
HIP   … Hipparcos catalogue number
ra   … Right ascension in degrees
dec   … Declination in degrees
Vmag   … Apparent magnitude in the V-band
tpm   … Total proper motion in milliarcseconds per year
pm in ra … Proper motion in right ascension direction in milliarcseconds per year
pm in dec … Proper motion in declination direction in milliarcseconds per year

Nr.	HIP	ra (deg)	dec (deg)	Vmag	tpm (mas/yr)	pm in ra (mas/yr)	pm in dec (mas/yr)
1.1	104217	316.717	38.734	6.05	5172.4	4107.40	3143.72
1.2	104214	316.712	38.741	5.20	5280.65	4155.10	3258.90
2	114622	348.311	57.168	5.57	2095.24	2074.37	294.97
3	115332	350.407	17.294	11.70	1485.52	-536.53	-1385.25
4	117473	357.300	2.404	8.98	1388.44	995.12	-968.25
5	1475	4.586	44.022	8.09	2917.95	2888.92	410.58
6	3821	12.271	57.817	3.46	1222.71	1087.11	-559.65
7	5336	17.054	54.924	5.17	3776.76	3421.44	-1599.27
8	171	0.540	27.084	5.80	1204.26	778.59	-918.72
9	3829	12.288	5.395	12.37	2977.84	1233.05	-2710.56
10	3765	12.094	5.283	5.74	1370.04	758.04	-1141.22
11	4856	15.621	71.681	9.98	1786.66	1745.69	-380.43
12	5247	16.776	63.941	9.00	1580.79	1548.21	319.28

2.2 Identification of the stars

Before taking an image of a star the telescope had to be pointed at the correct sky region. The coordinates were used as input for the program that is moving the telescope. Then an image was taken and compared to an existing image retrieved from the SIMBAD Astronomical Database. Usually those images looked very different. The orientation didn't fit and the star was either somewhere at the edge of the image or nowhere to be seen. Especially the high proper motion was a severe complication. Therefore, we had to look for similar stellar patterns in the images. Once some asterisms were identified, the telescope was moved a few arcminutes in the right direction. Soon the star was successfully placed near the center of the image. Additionally the images were rotated and flipped. The offsets are listed in the table below.

2.3 Settings and Circumstances

The images were taken using a V-band filter and a focus of 4.77mm.

Table 2.3: Settings and circumstances

Nr.   … Identifier
Date   … Observation date
T   … Outside temperature
RH   … Outside relative humidity
Sky   … Cloudiness
HIP   … Hipparcos catalogue number
ra   … Right ascension in (h min sec)
dec   … Declination in (° ' ")
Offset   … Offset from the given position

Nr	Date	T	RH	Sky	HIP	ra (h min sec)	dec (° ' ")	Offset
1	23.11.2017	9.1°C	66%	Many cirrus clouds	104217	21 06 55,3	38 44 31	5'E 2'S
					104214			
2					114622	23 13 17,0	57 10 06	6'E 4'S
3					115332	23 21 37,4	17 17 25	5'E
4					117473	23 49 12,5	02 24 04	5'E
5					1475	00 18 22,9	44 01 23	5E
6	6.12.2017	1.6°C	77%	Clear	3821	00 49 06,3	57 48 55	0
7					5336	01 08 16,4	54 55 13	2'E 1'S
8					171	00 02 10,2	27 04 56	2'E
9					3829	00 49 09,9	5 23 19	2'E
10					3765	00 48 23,0	5 16 50	2'E
11					4856	01 02 32,2	71 40 47	0
12					5247	01 07 08,2	63 56 29	0

3. Analysis

3.1. Data reduction

Before we can analyze the images, we must reduce noise and other disturbances. Additionally to the raw frame we need a bias frame, a dark frame and a flat field. The bias frame is created by closing the shutter of the camera and taking an image with zero exposure time. It provides the camera's offset in the signal and allows to determine the readout noise. The dark frame has the same exposure time as the raw frame, but the shutter is also closed. It shows the thermal noise and also contains the bias. The flat field is an image of an evenly illuminated area and is useful for testing the sensitivity of the pixels and contains the dark current and the bias. Our flatfield was obtained by observing the eastern sky after sunset.

From the original image the Masterdark was subtracted, which is the median of 5 or 10 dark frames. Then the image was divided by the Masterflat, which is the median of 10 flat fields, from which the Masterdark had been subtracted. The final step is to remove bad pixels by looking for outliers.
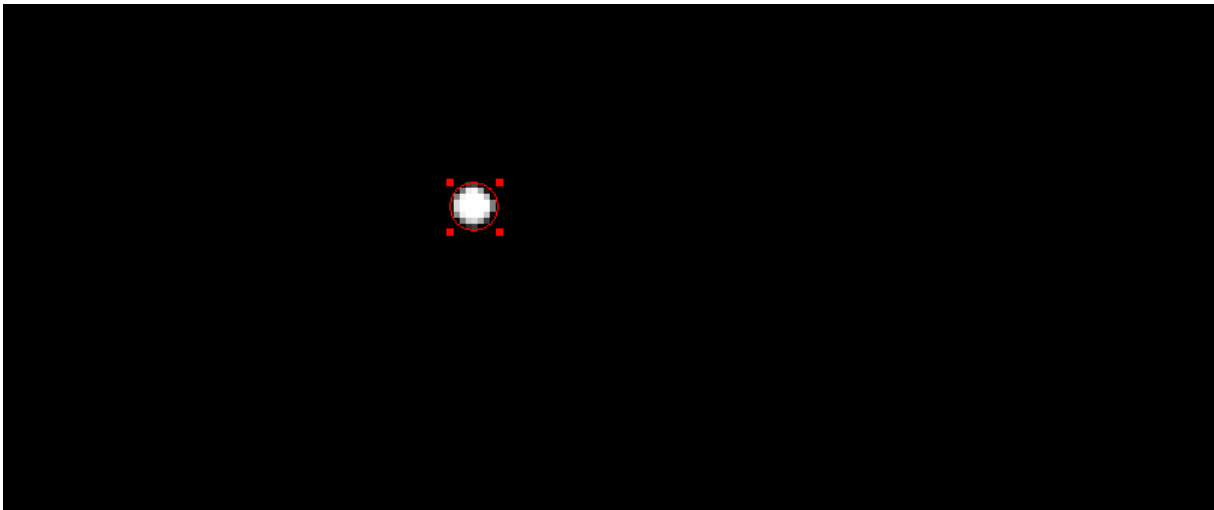
3.2. Determination of the position

To determine the exact positions of the objects, the program SAO – DS9 was used. Before analyzing the data, we used "astrometry.org" to create a coordinate system for each image. "astrometry.org" uses the positions of the visible stars in the image to derive an astrometric solution. Then there are 2 methods that have been used for gaining results with the least uncertainties.

The first is based on the "line"-function of SAO – DS9. As seen on Fig. 4.2.1, the stars on the image have diffraction spikes. One could argue that the exact position of the star is most likely at the intersection of these spikes. So by drawing two straight lines (blue lines in Fig. 4.2.1) exactly on the spikes and reading out the coordinates of the intersection, it is possible to get a good estimate of the position of the star. This method is only applicable to bright stars.

The second method uses the "circle"- and "centroid"-functions of the program. First the brightness and contrast have to be set, so that only the brightest part of the object remains visible. This leads to a higher accuracy. The star will now approximately appear as a disc as in Fig. 4.2.2. Then a circle (blue) is drawn around this disc. Using the "centroid"-function the circle is placed to match the disc. One can then read out the coordinates of the center of the circle, which should also be the center of the disc. Both figures show the same star.
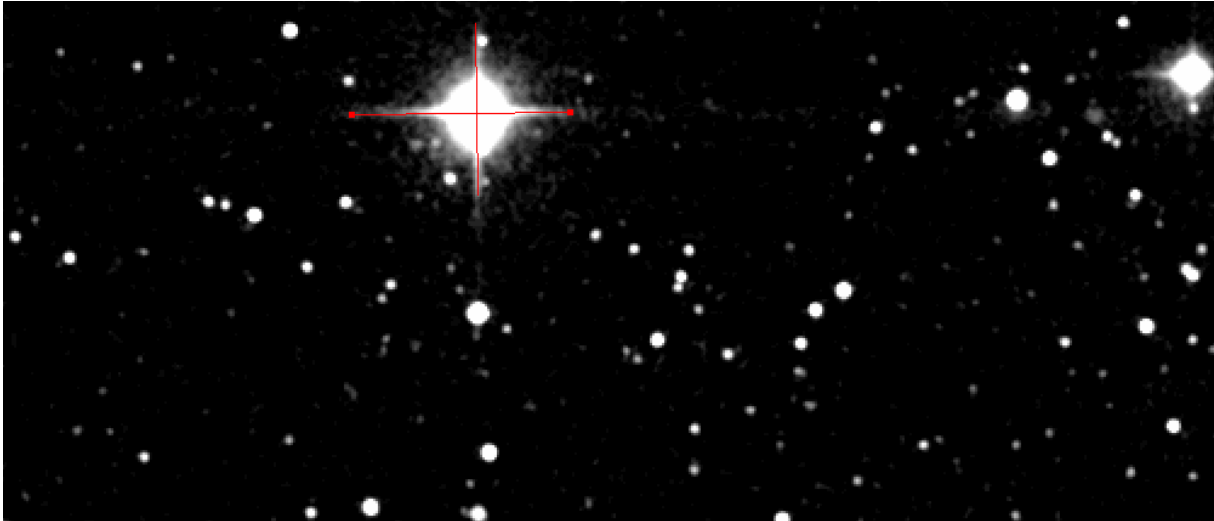
Fig 4.2.1: Determining the position of a star using the "line"-function of SAO – DS9

Fig 4.2.2: Determining the position of a star using the "circle"-function of SAO – DS9

3.3. Calculation of distances and velocities

To determine proper motions of the observed stars the positions were compared to those of earlier observations. SAO – DS9 has a built-in function which retrieves data from some servers and displays the images. To make sure that the retrieved image shows the same region of the sky, these images can be put on top of each other as an RGB image. Fig. 4.3. shows the three different epochs in red, green and blue on top of each other. The blue image was taken in the year 1954(DSS1), the green one in 1989(2MASS) and the red one was taken in 2017 for this Bachelor thesis. The stars, that didn't move much add up to a white color and the object of interest is seen in the three colors at three different positions. One can see how the resolution became better in time by comparing the apparent sizes of the same star in different epochs.
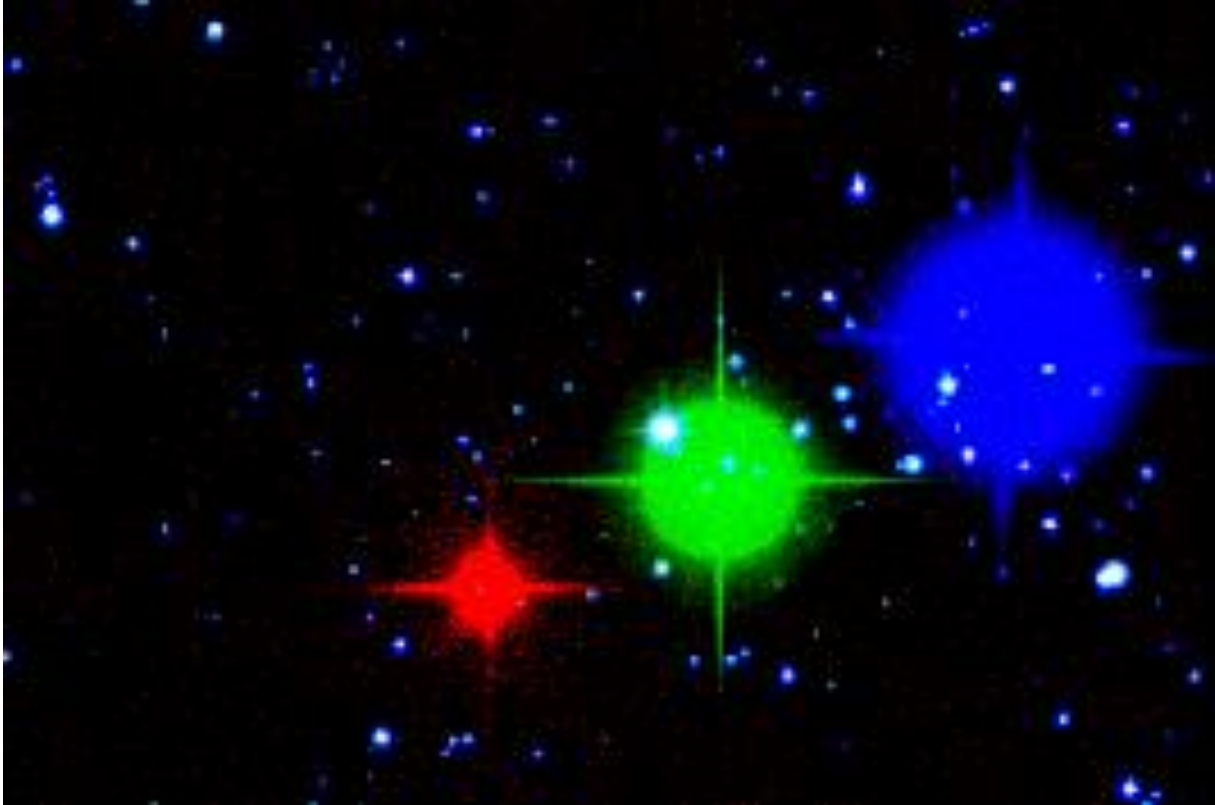
Fig. 4.3: Star N°7 in 1954 from SAO – DSS Server in blue, 1989 from IPAC – 2MASS Server in green and 2017 from our measurements in red

Now that it was ensured, that we identified and measured the right star, we are able to determine the positions of the star at different times with the methods described in Chapter 3.2. The following table shows an example of the results of one such measurement for star N°2.

Table 3.3: Positions of the star N° 2

Source   … Source of the image
Date   … Observation date
α   … Right ascension in (h min sec)
Δα   … Uncertainty of right ascension in ''
δ   … Declination in (° ' '')
Δδ   … Uncertainty of declination in ''

Source	Date	α	α in ''	Δα	δ	δ in ''	Δδ
DSS1	16.09.1952	23 13 5.140	1253777.10	4.5	57 9 52.00	205792.00	5
DSS2	16.09.1993	23 13 15.303	1253929.55	4.5	57 10 4.38	205804.38	3
2MASS	14.11.1999	23 13 16.867	1253953.01	1.5	57 10 6.03	205806.03	1
OLG	23.11.2017	23 13 21.482	1254022.23	1.5	57 10 12.01	205812.01	1

Tables with the measured positions of each star can be found in the appendix.

4. Results

The velocities of the stars were calculated as has been shown in Chapter 1.1. and the uncertainties are discussed in Chapter 5.1. The following table shows the results again for star N°2:

Table 4.1: distances and velocities of star N°2

Date 1	… Date of the first observation
Date 2	… Date of the second observation
t	… Time difference in days
d	… Angular distance in ''
Δd	… Uncertainty of the distance in ''
v	… Total angular velocity in ''/a
Δv	… Uncertainty of the angular velocity in ''/a
vδ	… Declination component of the angular velocity in ''/a
Δvδ	… Uncertainty of the declination component of the angular velocity in ''/a
vα	… Right ascension component of the angular velocity in ''/a
Δvα	… Uncertainty of the right ascension component of the angular velocity in ''/a

Date 1	Date 2	t	d	Δd	v	Δv	vδ	Δvδ	vα	Δvα
16.09.1952	16.09.1993	14975	84	15	2.0	0.4	0.3	0.2	2.0	0.15
16.09.1993	14.11.1999	2250	13	9	2.1	1.5	0.3	0.6	2.1	0.7
14.11.1999	23.11.2017	6584	38	5	2.1	0.3	033	0.11	2.09	0.11
16.09.1952	23.11.2017	23809	135	10	2.07	0.15	0.31	0.09	2.05	0.06

Tables with the velocities of each star can be found in the appendix.

The last row of Table 4.1 shows the results for the longest time period. One can see that the uncertainties here are the smallest. Note that all velocities are average velocities for the chosen time interval. Therefore, it is not necessary that they all have the same value and they could even differ from the results from the Gaia and Hipparcos missions. We will see that this is not the case. The following table shows a comparison of our results with the longest interval and satellite data for star N°2:

Table 4.2: velocities of star N°2 with server data

OLG	… Observatory Lustbühel, our data
HIP	… Data from the Hipparcos catalogue
GAIA	… Data from the Gaia catalogue

Source	v	vδ	vα
OLG	2.07 ± 0.15	0.31 ± 0.09	2.05 ± 0.06
HIP	2.09524	0.29497	2.07437
GAIA	2.09537778	0.294936	2.074517

As we can see in table 4.2 the values for the velocities of star N°2 match the satellite data. This is the case for every chosen star. The next table shows the results for the velocities for every star, always using the longest time interval. Note that instead of star N°5 there are now star N°5.1 and N°5.2, because during analysis we noticed that this is a double star, so it was included in the calculations.

Table 4.3: velocities of the stars for the longest time interval

Nr.	v in "/a	Δv in "/a	vδ in "/a	Δvδ in "/a	vα in "/a	Δvα in "/a
1.1	5.3	1.0	3.2	0.5	4.2	0.3
1.2	5.2	1.0	3.1	0.5	4.1	0.3
2	2.1	0.2	0.3	0.1	2.05	0.06
3	1.5	0.1	-1.38	0.02	-0.54	0.05
4	1.4	0.2	-0.97	0.05	1.00	0.09
5.1	2.9	0.3	0.4	0.1	2.9	0.1
5.2	2.9	0.1	0.34	0.03	2.87	0.06
6	1.3	0.5	-0.6	0.2	1.2	0.2
7	3.8	0.4	-1.6	0.2	3.5	0.2
8	1.5	0.6	-1.2	0.2	0.8	0.2
9	3.0	0.1	-2.71	0.02	1.22	0.05
10	1.4	0.6	-1.2	0.2	0.8	0.3
11	1.9	0.2	-0.4	0.1	1.8	0.1
12	1.6	0.2	0.30	0.05	1.57	0.08

These velocities have been compared to Hipparcos and Gaia data. The following plots show the comparison to Hipparcos data only, because the difference between Gaia and Hipparcos are negligible for the achieved precision.

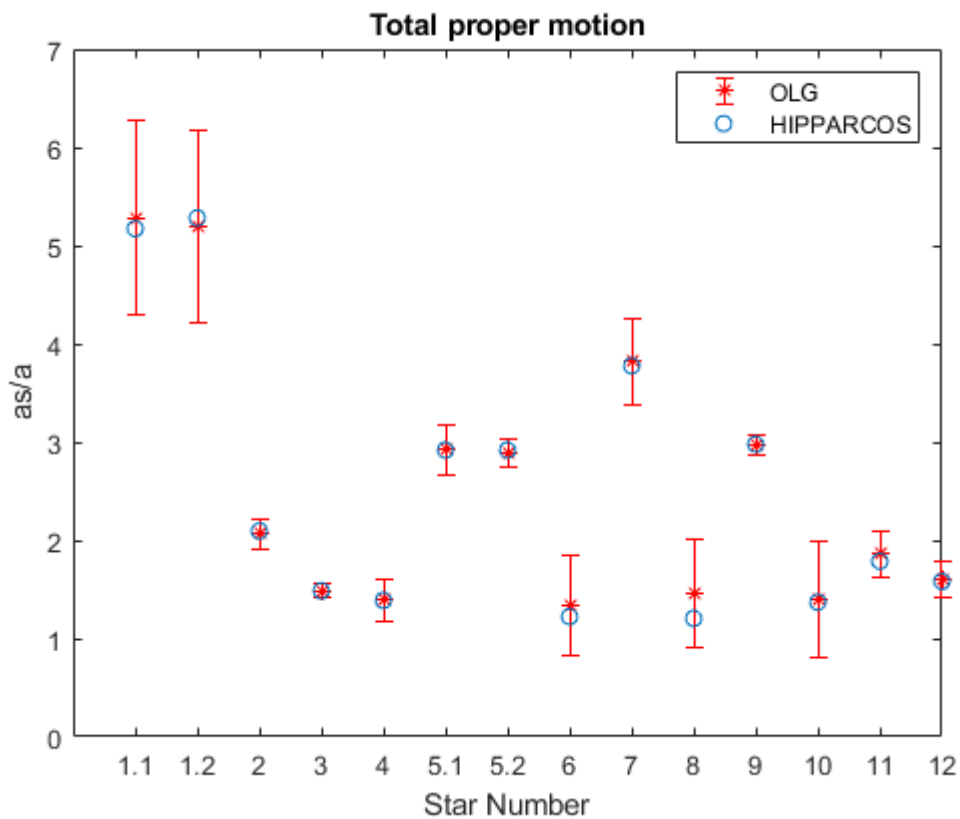Fig. 4.1: The total velocities of the stars. OLG stands for observatory Lustbühel Graz and represents our data.
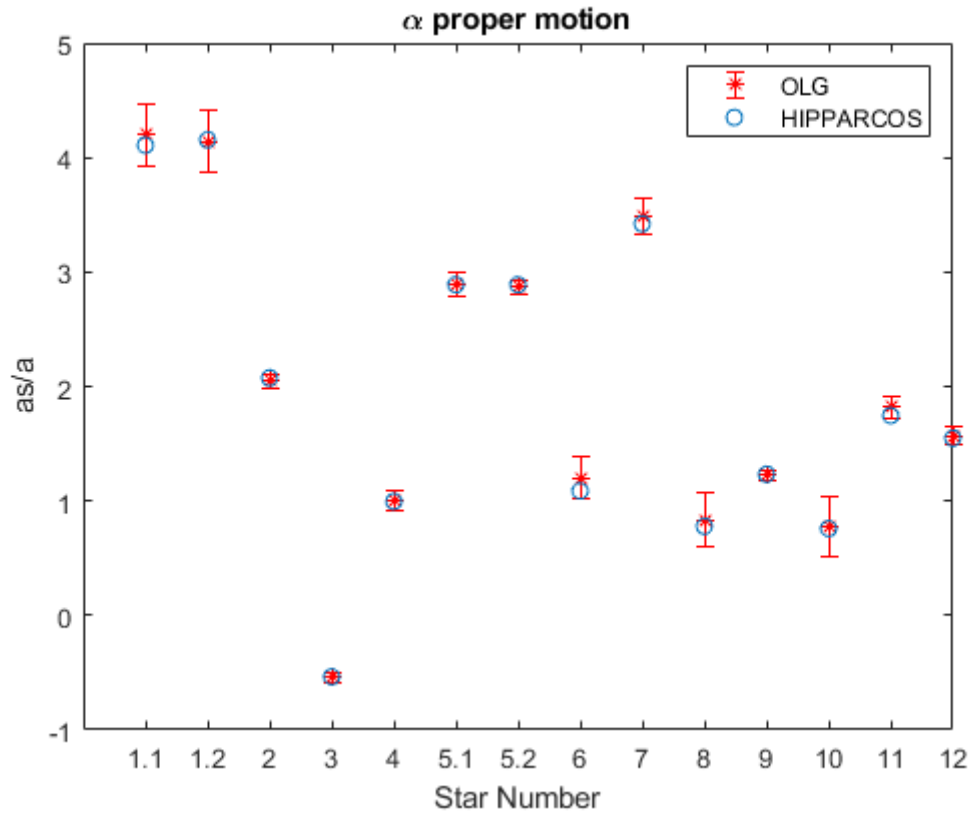
Fig. 4.2: The velocities of the stars in right ascension. OLG stands for observatory Lustbühel Graz and represents our data.
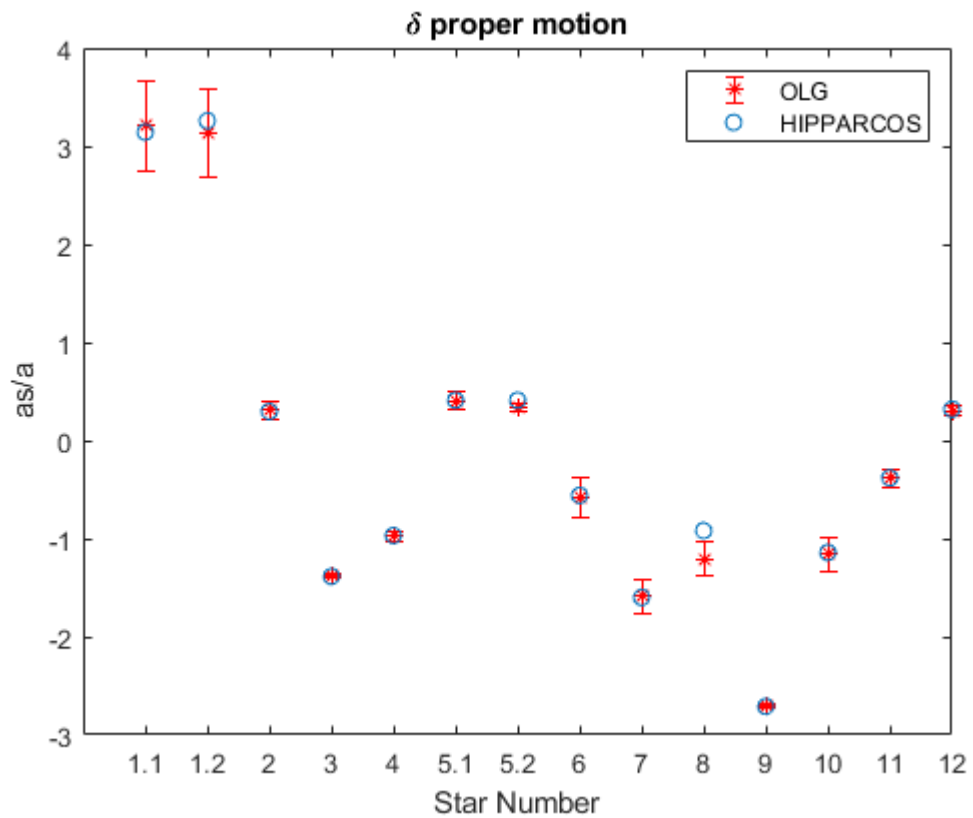

Fig. 4.3: The velocities of the stars in declination. OLG stands for observatory Lustbühel Graz and represents our data.

We see that the satellite data matches our results very well.

One could expect that the angular velocity decreases with the distance of the star. In the following plot we see again the total velocity of the stars, but now they are arranged by parallax.
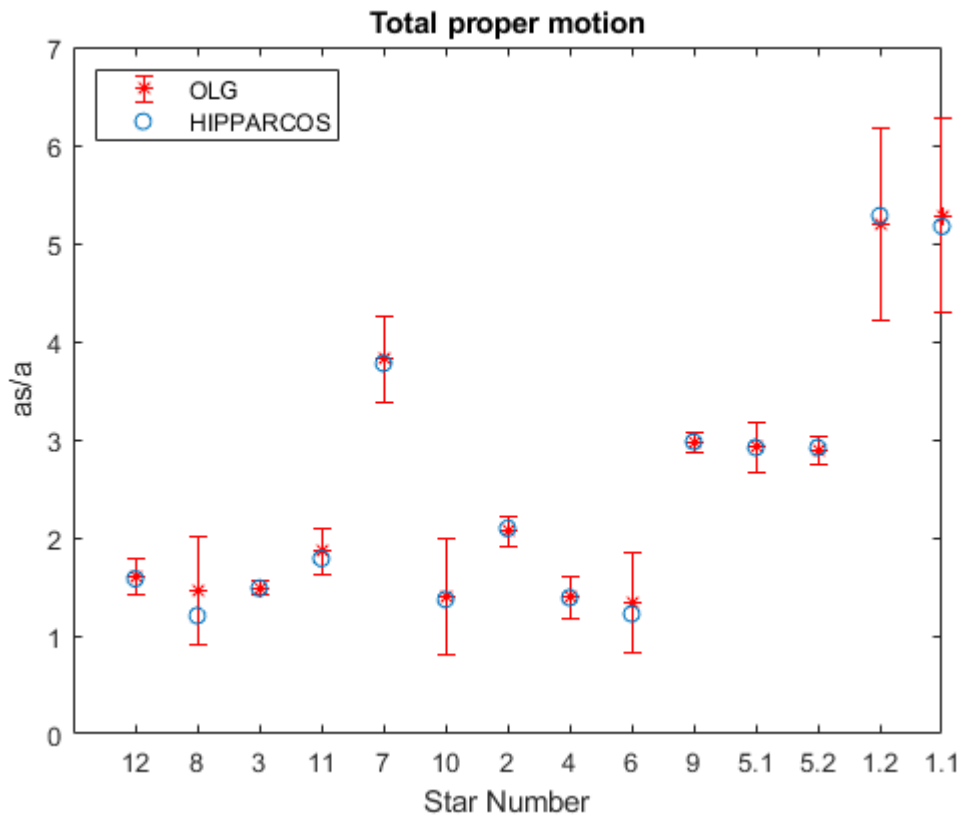

Fig. 4.4: The total velocities of the stars with ascending parallax. OLG stands for observatory Lustbühel Graz and represents our data.

In Fig. 4.4 we roughly see that such a trend does exist. Note that the x-axis is not linear but equally spaced between the stars and the stars on the right are closest to us.

5. Discussion

5.1. Uncertainty estimation

Since the stellar light is distributed on the detector over an area with many pixels, the uncertainty in the measurement is larger than the pixel size of the camera. The exact position of the star could be anywhere in that area, but, if the area is circular, the star is most likely in the center of the circle. More precisely, "circle" describes here the area of pixels with values above background level. It wouldn't make much sense to declare the whole area of the circle to be the uncertainty of the position, because it is very unlikely that the star is located somewhere on the outer parts of the circle. As explained in Chapter 3.2. we can also use the diffraction spikes to determine the position. When comparing the results of the two methods, we saw that the distance between the positions gathered from each method is much smaller than the radius of the circle. This indicates again that it wouldn't be useful to take the whole circle as uncertainty. We estimate the uncertainty to be one third of the radius of the circle. The intersection of the diffraction spikes was always inside of this limit, so we decided, that it is a reasonable estimate.

Another source for uncertainties could be the parallax motion, but the uncertainties from above are already greater than the parallax angles of the stars.

To determine how the uncertainty propagates in the calculation, linear error propagation was used:

$$\Delta f = \sum_i \left| \frac{\partial f}{\partial x_i} \right| \Delta x_i$$

Contrary to Gauss's error propagation, which requires statistical errors, linear error propagation is commonly used to find the maximum error for the value of f with independently measured quantities x_i and their estimated errors Δx_i. This formula originates from the Taylor expansion of f, where only the linear term is considered. Therefore Δx_i should be small, compared to x_i.

In our context, we measured distances d_α and d_δ with their estimated uncertainties Δd_α and Δd_δ and calculated the total distance d with

$$d = \sqrt{(d_\alpha \cdot \cos(\delta))^2 + d_\delta^2},$$

leading to an uncertainty of

$$\Delta d = \left| \frac{\partial d}{\partial d_\alpha} \right| \Delta d_\alpha + \left| \frac{\partial d}{\partial d_\delta} \right| \Delta d_\delta = \frac{2 d_\alpha \cdot \cos(\delta)^2}{\sqrt{(d_\alpha \cdot \cos(\delta))^2 + d_\delta^2}} \Delta d_\alpha + \frac{2 d_\delta}{\sqrt{(d_\alpha \cdot \cos(\delta))^2 + d_\delta^2}} \Delta d_\delta.$$

Linear error propagation was also applied to the calculation of the average velocities of the stars.

5.2. Accelerations

Often, while calculating velocities for one star in different time intervals, it looked like there was a trend. Sometimes the velocity looked like going steadily up in time. This sparked the idea of calculating the angular accelerations as well and maybe even finding a $\cos$ – pattern, meaning that the star would orbit some other object. This has been tried for star N°2, because it shows the most promising pattern.
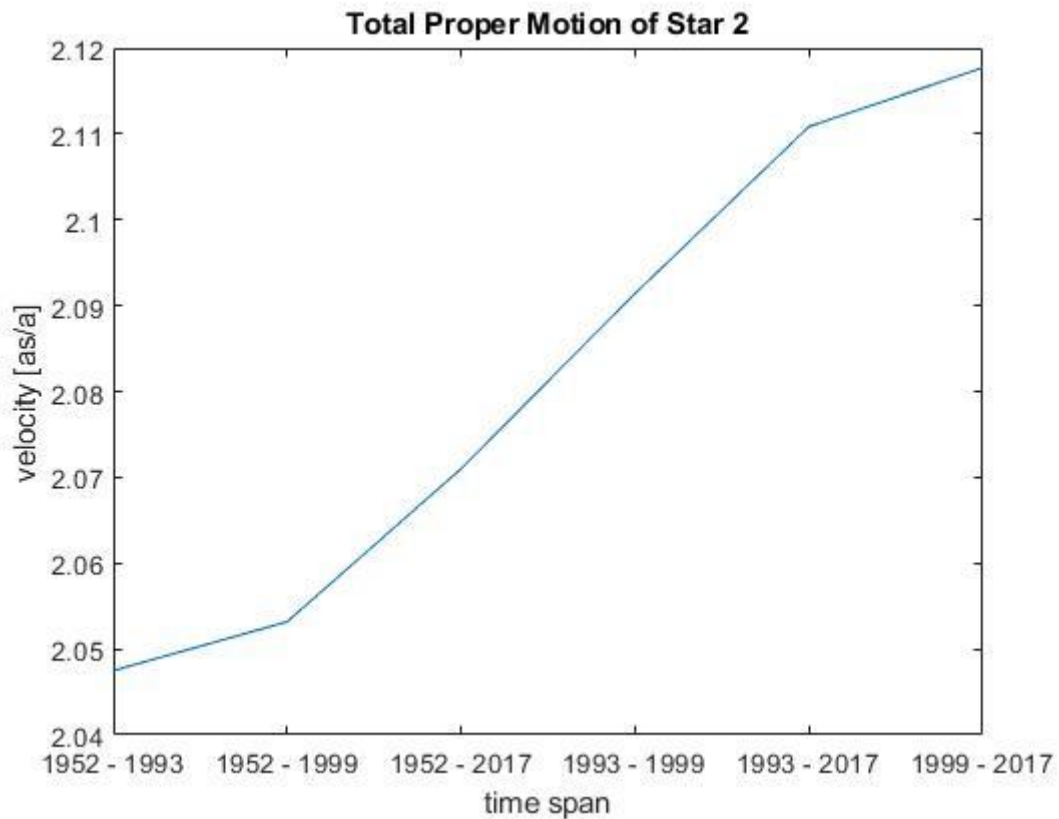
Fig.5.2.1: Total velocities of star N°2 for different time intervals

In Fig. 5.2.1 the time intervals are sorted by increasing average observation date. The timeline therefore is not linear. Still we see a very convincing pattern, the velocity appears to steadily increase. To verify this, we might look at the right ascension and declination components of this movement.

Fig. 5.2.2: Velocities of star N°2 in right ascension direction for different time intervals

Fig. 5.2.3: Velocities of star N°2 in declination direction for different time intervals

In right ascension we see a very similar pattern, it even has a similar curvature. In declination we don't see it. One could argue that the proper motion in declination direction is generally much smaller and doesn't have to follow the same pattern exactly. Furthermore, if we ignore the value at the time span between 1993 and 1999, we still have an increasing function. It wouldn't be unlikely that there is an error at this point, because the time span is very short. Now we could conclude, that star N°2 has a steady positive acceleration, but we didn't consider the uncertainties of our velocities yet. Here is the total proper motion of star N°2 with uncertainties:
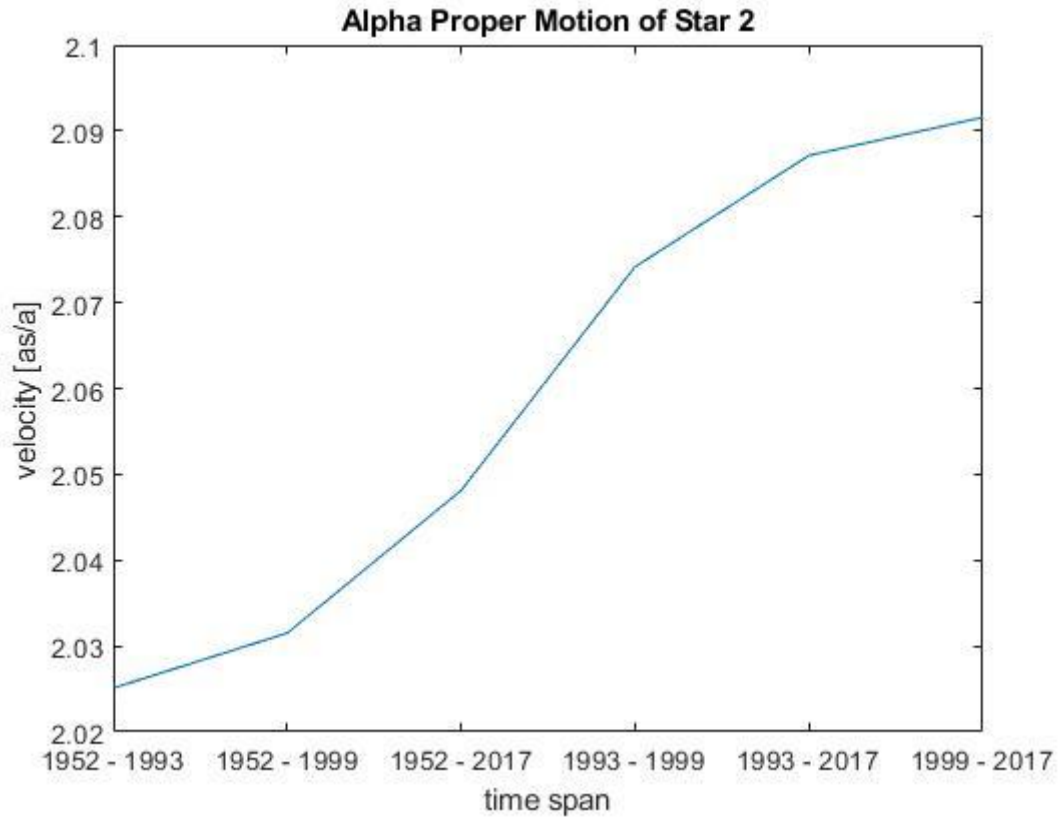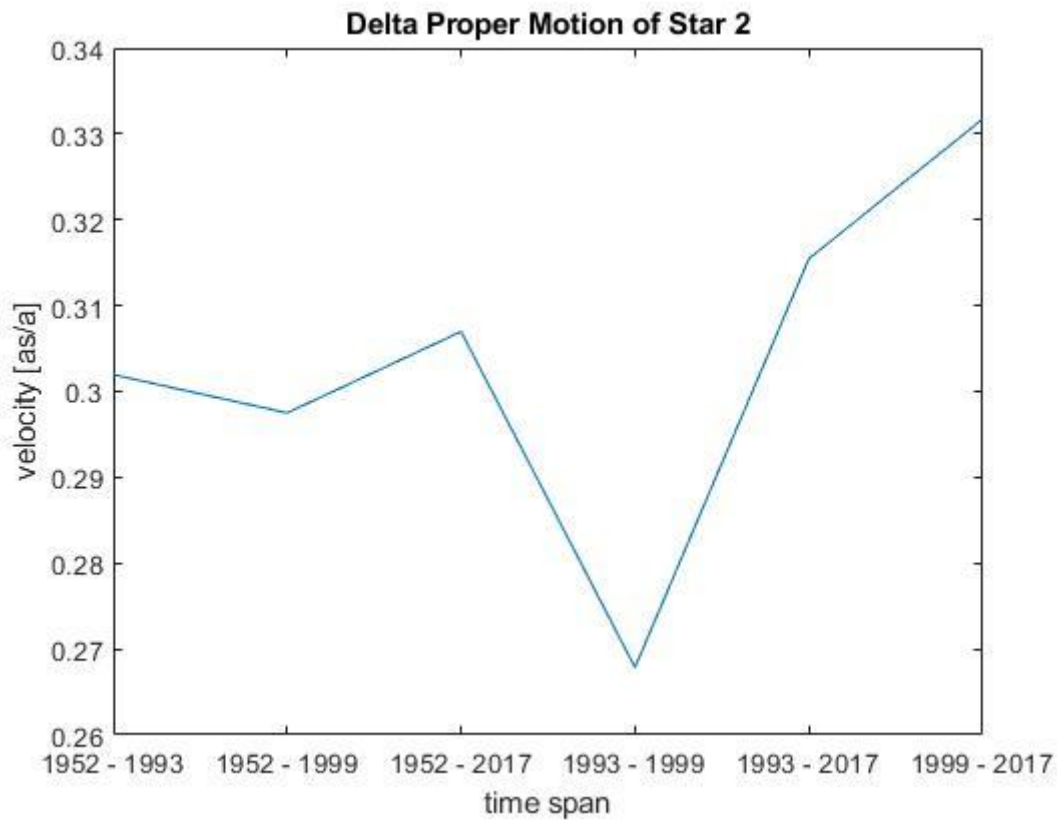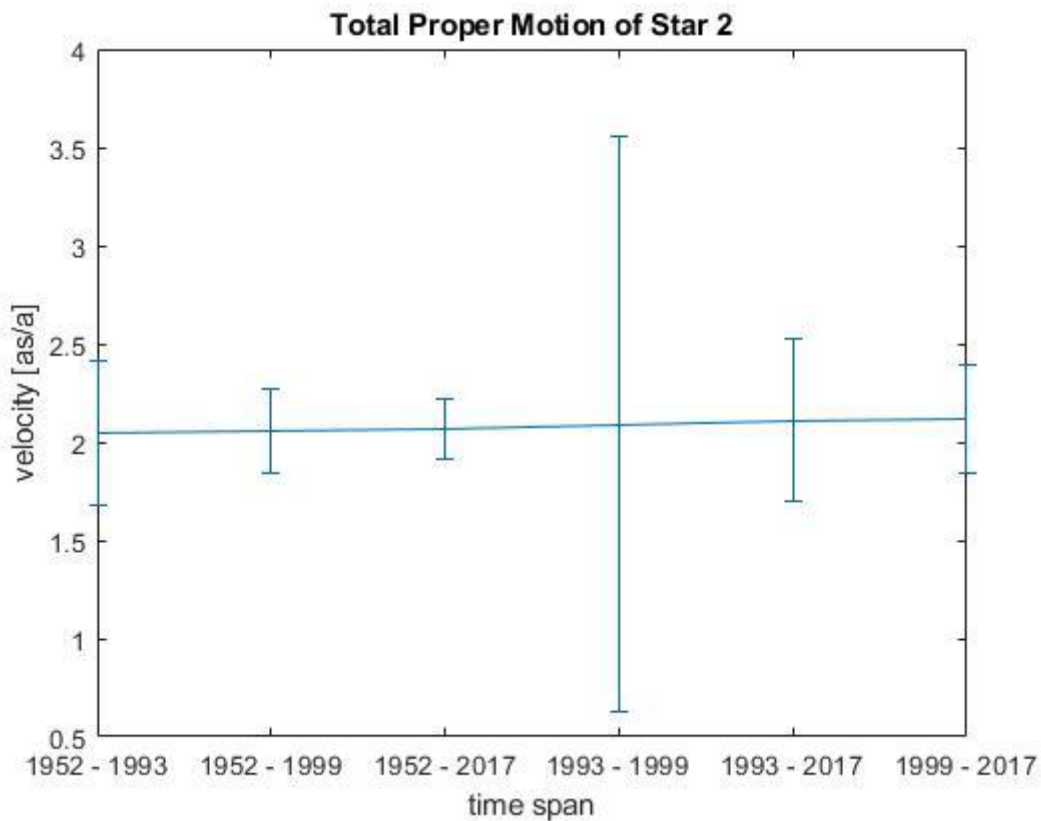

Fig. 5.2.4: Total velocities of star N°2 for different time intervals with uncertainties

We see, that interpreting a pattern into this is very unscientific. The plots of the right ascension and declination components with uncertainties look similar. We also see, that the uncertainty between 1993 and 1999 is very big, because of the short time span. If there was a significant acceleration as in Fig 6.2.1, the values for the proper motion from Gaia should be approximately 0.03 as/a higher than from Hipparcos. The actual difference is 0.00014 as/a.

When analyzing 14 different stars it is very likely, that at least one shows an interesting pattern within the uncertainty intervals by chance. This is what happened here. To conclude, there is no significant acceleration in our data.

Since there are 2 binaries in our observation, we also looked for signs of orbital motion. If there were differences in the proper motion between the two stars of a binary system, one might calculate an orbital velocity. But, similar to the discussion about accelerations, there were no significant results.

6. Conclusion

Despite having a much lower precision than the satellite missions Gaia and Hipparcos, we were able to reproduce the proper motion of 14 stars. In Fig 4.4 one can see, that our results match the satellite data very well. We also noticed, that the proper motion of the stars roughly decreases with their distance to earth. The most important components to the accuracy of our measurement are the long timelines that we worked with. We had the opportunity to use data from the early fifties, published by the Digital Sky Survey, which lead to a very low uncertainty in the average velocities. Fig. 5.2.4 shows how the time span affects the uncertainty. The error bar at "1993 – 1999" is by far the largest with the shortest time interval, whereas "1954 – 2017", which is the smallest and has the largest time interval. Of course, the resolution also of the data had an influence on the accuracy of the measurement, but the time interval had a bigger influence. To take parallax and orbital motion into account, however, requires much higher precision of the individual measurement.

References

Gaia Collaboration et al. (2016, 8 16). The Gaia Mission. *Astronomy & Astrophysics*.

Hanslmaier, A. (2014). *Einführung in die Astronomie und Astrophysik.* Graz: Springer Spektrum.

M.F. Skrutskie et al. (2006, 2). The Two Micron All Sky Survey (2MASS). *The Astronomical Journal*.

McLean et al., B. J. (2000). The Status of the Second Generation Digitized Sky Survey and Guide Star Catalog.

Mikulski Archive for Space Telescopes. (2018, 8. 15). Retrieved from https://archive.stsci.edu/dss/

Morrison, J. (1995). Accessing the Digitized Sky Survey. *ASP Conference Series*.

Perryman, M. (2012, 10 8). The history of astrometry. *The European Physics Journal H*.

Perryman, M. A. (1997). *The Hipparcos and Tycho catalogues: Astrometric and photometric star catalogues derived from the ESA Hipparcos Space Astrometry Mission.* Noordwijk, Netherlands: ESA Publications Division.

Appendix

Table A.1.1: distances and velocities of star N°1.1

Date 1 … Date of the first observation
Date 2 … Date of the second observation
t … Time difference in days
d … Angular distance in ''
Δd … Uncertainty of the distance in ''
v … Total angular velocity in ''/a
Δv … Uncertainty of the angular velocity in ''/a
vδ … Declination component of the angular velocity in ''/a
Δvδ … Uncertainty of the declination component of the angular velocity in ''/a
vα … Right ascension component of the angular velocity in ''/a
Δvα … Uncertainty of the right ascension component of the angular velocity in ''/a

Date 1	Date 2	t	d	Δd	v	Δv	vδ	Δvδ	vα	Δvα
09.07.1951	07.09.1991	14670	210	87	5.2	2	3.2	1	4.2	0.6
07.09.1991	20.06.1998	2478	37	66	5.4	10	3.4	4	4.2	2.7
20.06.1998	23.11.2017	7096	103	44	5.3	2	3.2	1	4.2	0.6
09.07.1951	23.11.2017	24244	350	66	5.3	1	3.2	0.5	4.2	0.3

Table A.1.2: distances and velocities of star N°1.2

Date 1	Date 2	t	d	Δd	v	Δv	vδ	Δvδ	vα	Δvα
09.07.1951	07.09.1991	14670	210	87	5.2	2	3.1	1	4.1	0.6
07.09.1991	20.06.1998	2478	37	66	5.4	10	3.3	4	4.2	2.7
20.06.1998	23.11.2017	7096	103	44	5.2	2	3.2	1	4.1	0.6
09.07.1951	23.11.2017	24244	350	66	5.2	1	3.1	0.5	4.1	0.3

Table A.2: distances and velocities of star N°2

Date 1	Date 2	t	d	Δd	v	Δv	vδ	Δvδ	vα	Δvα
16.09.1952	16.09.1993	14975	84	15	2.0	0.4	0.3	0.2	2.0	0.15
16.09.1993	14.11.1999	2250	13	9	2.1	1.5	0.3	0.6	2.1	0.7
14.11.1999	23.11.2017	6584	38	5	2.1	0.3	033	0.11	2.09	0.11
16.09.1952	23.11.2017	23809	135	10	2.07	0.15	0.31	0.09	2.05	0.06

Table A.3: distances and velocities of star N°3

Date 1	Date 2	t	d	Δd	v	Δv	vδ	Δvδ	vα	Δvα
12.08.1951	13.08.1951	1	0	9	200	3000	60	800	-200	2000
13.08.1951	29.09.1997	16849	68	5	1.5	0.1	-1.38	0.03	-0.53	0.07
29.09.1997	23.11.2017	7360	30	3	1.5	0.1	-1.39	0.04	-0.56	0.10
12.08.1951	23.11.2017	24210	99	5	1.5	0.1	-1.38	0.02	-0.54	0.05

Table A.4: distances and velocities of star N°4

Date 1	Date 2	t	d	Δd	v	Δv	vδ	Δvδ	vα	Δvα
28.11.1951	29.11.1951	1	0	23	80	8000	25	2000	80	4000
29.11.1951	15.08.2000	17792	69	16	1.4	0.3	-1.01	0.08	1.01	0.14
15.08.2000	23.11.2017	6309	23	7	1.3	0.4	-0.88	0.09	0.96	0.17
28.11.1951	23.11.2017	24102	92	14	1.4	0.2	-0.97	0.05	1.00	0.09

Table A.5.1: distances and velocities of star N°5.1

Date 1	Date 2	t	d	Δd	v	Δv	vδ	Δvδ	vα	Δvα
04.10.1954	03.10.1954	-1	0	25	80	9000	-70	3000	-40	4000
03.10.1954	04.11.1998	16103	129	14	2.9	0.3	0.41	0.09	2.89	0.14
04.11.1998	23.11.2017	6959	56	7	2.9	0.4	0.41	0.07	2.90	0.16
04.10.1954	23.11.2017	23061	184	16	2.9	0.3	0.41	0.08	2.89	0.11

Table A.5.2: distances and velocities of star N°5.2

Date 1	Date 2	t	d	Δd	v	Δv	vδ	Δvδ	vα	Δvα
04.10.1954	03.10.1954	-1	0	25	150	4000	-70	1000	-100	2000
03.10.1954	04.11.1998	16103	129	14	2.9	0.2	0.34	0.03	2.88	0.07
04.11.1998	23.11.2017	6959	56	7	2.9	0.3	0.35	0.04	2.87	0.11
04.10.1954	23.11.2017	23061	184	16	2.9	0.2	0.34	0.03	2.87	0.06

Table A.6: distances and velocities of star N°6

Date 1	Date 2	t	d	Δd	v	Δv	vδ	Δvδ	vα	Δvα
16.09.1952	01.09.1989	13499	47	37	1.3	1.0	-0.4	0.4	1.2	0.4
01.09.1989	13.01.2000	3786	18	23	1.8	2.2	-1.2	0.8	1.3	0.8
13.01.2000	06.12.2017	6537	23	17	1.3	1.0	-0.5	0.3	1.1	0.3
16.09.1952	06.12.2017	23822	87	33	1.3	0.5	-0.6	0.2	1.2	0.2

Table A.7: distances and velocities of star N°7

Date 1	Date 2	t	d	Δd	v	Δv	vδ	Δvδ	vα	Δvα
04.01.1954	28.08.1989	13020	135	38	3.8	1.1	-1.6	0.4	3.4	0.4
28.08.1989	29.12.1998	3410	37	19	4.0	2.0	-1.6	0.8	3.7	0.8
29.12.1998	06.12.2017	6917	72	8	3.8	0.4	-1.6	0.2	3.5	0.2
04.01.1954	06.12.2017	23347	245	28	3.8	0.4	-1.6	0.2	3.5	0.2

Table A.8: distances and velocities of star N°8

Date 1	Date 2	t	d	Δd	v	Δv	vδ	Δvδ	vα	Δvα
08.12.1950	23.08.1993	15599	54	67	1.3	1.6	-1.0	0.5	0.8	0.7
23.08.1993	03.10.1998	1867	7	39	1.4	7.6	-0.9	2.2	1.1	3.1
03.10.1998	06.12.2017	7004	38	8	2.0	0.4	-1.8	0.1	0.8	0.2
08.12.1950	06.12.2017	24470	98	37	1.5	0.6	-1.2	0.2	0.8	0.2

Table A.9: distances and velocities of star N°9

Date 1	Date 2	t	d	Δd	v	Δv	vδ	Δvδ	vα	Δvα
31.10.1953	31.10.1953	0	0	-	-	-	-	-	-	-
31.10.1953	12.08.2000	17087	139	8	3.0	0.2	-2.69	0.04	1.25	0.09
12.08.2000	06.12.2017	6325	52	6	3.0	0.3	-2.76	0.09	1.14	0.17
31.10.1953	06.12.2017	23412	190	6	2.97	0.09	-2.71	0.02	1.22	0.05

Table A.10: distances and velocities of star N°10

Date 1	Date 2	t	d	Δd	v	Δv	vδ	Δvδ	vα	Δvα
31.10.1953	30.08.1994	14913	58	51	1.4	1.2	-1.2	0.4	0.8	0.6
30.08.1994	13.08.2000	2175	9	22	1.5	3.7	-1.2	1.0	0.9	1.7
13.08.2000	06.12.2017	6324	23	8	1.3	0.5	-1.1	0.1	0.7	0.2
31.10.1953	06.12.2017	23412	89	38	1.4	0.6	-1.2	0.2	0.8	0.3

Table A.11: distances and velocities of star N°11

Date 1	Date 2	t	d	Δd	v	Δv	vδ	Δvδ	vα	Δvα
23.09.1954	22.09.1954	-1	0	27	150	9000	65	4000	100	4000
22.09.1954	01.10.1999	16445	84	15	1.9	0.3	-0.39	0.13	1.82	0.13
01.10.1999	06.12.2017	6641	33	5	1.8	0.3	-0.38	0.08	1.79	0.11
23.09.1954	06.12.2017	23085	118	15	1.9	0.2	-0.38	0.09	1.82	0.10

Table A.12: distances and velocities of star N°12

Date 1	Date 2	t	d	Δd	v	Δv	vδ	Δvδ	vα	Δvα
10.01.1954	13.09.1995	15221	66	16	1.6	0.4	0.30	0.12	1.54	0.17
13.09.1995	07.01.1999	1212	6	9	1.7	2.7	0.2	0.8	1.7	1.2
07.01.1999	06.12.2017	6908	31	5	1.6	0.3	0.33	0.05	1.60	0.11
10.01.1954	06.12.2017	23341	102	12	1.6	0.2	0.30	0.05	1.57	0.08